

## Evolution of Raindrop Spectra with Collision-Induced Breakup

ROLAND LIST AND J. R. GILLESPIE

*Department of Physics, University of Toronto, Toronto, Ontario, Canada*

(Manuscript received 20 February 1976, in revised form 21 June 1976)

### ABSTRACT

A numerical model was set up to study the evolution of raindrop spectra by collision-induced breakup as measured in the laboratory. The main conclusion is that drops with diameters larger than 2–3 mm, falling in a population of smaller drops typical of natural rain, break up in comparatively short times (1–5 min in rainfalls of 100 mm h<sup>-1</sup>). The presence of large drops (4–6 mm) in (cold) rain produced by the Wegener-Bergeron-Findeisen mechanism through melting of ice particles can be attributed to the short time available for large drops to break up in sufficient numbers during the time of fall after melting. Large drops are scarce in (steady-state) warm rain because they break up in collisions and rarely reach diameters larger than 2.5 mm. Hence, the standard notion of a critical diameter of 5–6 mm which raindrops are supposed to reach before breakup due to aerodynamic instability is no longer acceptable.

### 1. Introduction

Langmuir (1948) gives a description of the mechanism by which warm rain (from clouds with temperatures greater than 0°C) forms through collection of smaller drops by larger ones in the same population. After some period of growth, these drops are assumed to approach an implied aerodynamic stability limit of ~6 mm and to break up into two or more fragments which are still large relative to the main population. Then these fragments continue their growth by accretion and may in turn break up, representing a "chain reaction" process. The recognition that the breakup mechanism is not likely to be aerodynamic was evident after one of the authors (R. L.) floated 15 mm diameter drops in the Swiss Hail tunnel in 1960 (unpublished); results from both experimental work (Pruppacher and Pitter, 1971) and theory (Klett, 1971) indicated that drops with equivalent spherical diameters as large as 10 mm are not disrupted aerodynamically. As originally proposed by Magarvey and Taylor (1956) and shown by McTaggart-Cowan and List (1975; hereafter M-L) and earlier calculations of mean free paths of raindrops (List *et al.*, 1970), breakup induced by collision with smaller drops must at present be considered as the key mechanism in the limitation of raindrop size. The experiments by M-L also provide data on the fragment size-distribution after collisions between selected drop pairs falling essentially vertically at their respective terminal speeds. Using this information it is possible to model the time evolution of an ensemble of drops, taking into account both coalescence and breakup due to collisions.

A further conclusion to be drawn from these investigations is that while coalescence of large drops (diameter  $D_L = 3\text{--}5$  mm) with smaller ones ( $D_S \geq 1$  mm) is a rare event, the most likely outcome of such a collision is the production of numerous fragments with loss of mass from the large participating drop or its disruption. Thus, the coalescence efficiency for these drops is much less than unity, the value usually adopted by modelers.

### 2. Mathematical model of the coalescence and breakup processes

Let  $P(m; \mu, \mu_1)dm$  denote the probability of obtaining a small drop in the mass range  $m$  to  $m+dm$  by collision and breakup of two drops with initial masses  $\mu$  to  $\mu+d\mu$  and  $\mu_1$  to  $\mu_1+d\mu_1$ . It is emphasized that  $P$  is a conditional probability, given that a collision had occurred. Using the assumption that the drops are distributed randomly in space, the rate of formation  $W(m, \mu)$  per unit of volume of drops of mass  $m$  from one single drop of mass  $\mu$  can be written as

$$W(m, \mu) = \pi \int_0^\mu n(\mu_1, t) (r_\mu + r_{\mu_1})^2 E_1(\mu, \mu_1) \times [V_T(\mu) - V_T(\mu_1)] P(m; \mu, \mu_1) d\mu_1, \quad (1)$$

where  $W(m, \mu)d\mu dm$  is the rate of formation of drops in the mass range  $m$  to  $m+dm$  by collision-induced breakup of drops in the range  $\mu$  to  $\mu+d\mu$ ;  $r_\mu$  and  $r_{\mu_1}$  are the radii of two interacting drops of masses  $\mu$  and  $\mu_1$  ( $\leq \mu$ ), respectively;  $E_1(\mu, \mu_1)$  is the collision

efficiency;  $n(\mu_1, t)d\mu_1$  is the number of drops with masses between  $\mu_1$  and  $\mu_1 + d\mu_1$  per unit volume at time  $t$ ; and  $[V_T(\mu) - V_T(\mu_1)]$  is the difference in terminal speeds of the two drops. Thus the factors in the integrand of (1) up to and including the difference of terminal speeds express the rate of collision of drops of mass  $\mu_1$  with a drop of mass  $\mu$ . When this rate is multiplied by the conditional probability  $P(m; \mu, \mu_1)$  the product expresses the average rate of formation of fragments with mass  $m$  in collisions of  $\mu$  and  $\mu_1$  drops. To obtain the final form of  $W(m, \mu)$  we must integrate over the range of masses of the smaller "incoming" drops  $\mu_1$ .

The conditional probability  $P(m; \mu, \mu_1)$  is the gateway into the model for the experimental data of M-L. How  $P$  is obtained from the observations of drop collisions is discussed later in Section 4.

The coalescence kernel  $K(\mu, m)$  is written in the usual form (Berry, 1967)

$$K(\mu, m) = \pi(r_\mu + r_m)^2 E_1(\mu, m) E_2(\mu, m) |V_T(\mu) - V_T(m)|, \quad (2)$$

where  $E_2(\mu, m)$  is the coalescence efficiency for colliding drops of masses  $\mu$  and  $m$ .

Let  $B(m, t)dm$  represent the rate of disappearance per unit of volume of drops of mass  $m$  to  $m + dm$  at time  $t$ . In this present model, breakup occurs only on collision of two drops; for arguments against aerodynamic breakup as described by Komabayasi *et al.* (1964) and modeled by Srivastava (1971), see M-L. Consequently, the breakup rate can be expressed as

$$B(m, t) = - \int_m^\infty n(\mu, t) W(m, \mu) d\mu + \frac{n(m, t)}{m} \times \int_0^m \mu W(\mu, m) d\mu. \quad (3)$$

The first term on the right represents the increase in number of  $m$  drops due to breakup of larger ones, whereas the second term gives the loss due to breakup of  $m$  drops (all fragment masses  $\mu$  have to be added up to give, when divided by  $m$ , the number of broken  $m$  drops).

If  $C(m, t)dm$  represents the net rate of production per unit of volume of drops of mass  $m$  to  $m + dm$  at time  $t$  by coalescence, then according to Twomey (1964) and Mordy and Berry (1965) the stochastic coalescence rate can be written

$$C(m, t) = \int_0^{m/2} n(\mu, t) n(m - \mu, t) K(\mu, m - \mu) d\mu - n(m, t) \int_0^\infty n(\mu, t) K(m, \mu) d\mu. \quad (4)$$

Then the coagulation equation is

$$\frac{dn(m, t)}{dt} = C(m, t) - B(m, t). \quad (5)$$

If the initial condition  $n(m, t=0) = n_0(m)$  is specified, then (5) can be used to compute the evolution of the drop-size spectrum. Here  $n_0(m)$  is a given function specifying the drop distribution at  $t=0$ . Melzak (1957) has studied equations of the form (5). Readers are referred to this work for the detailed mathematical conditions necessary to ensure that a unique solution exists. Briefly, the conditions on  $W$ ,  $K$  and  $n_0(m)$  are fulfilled if they are chosen to be non-negative continuous functions—which they should be on physical grounds.

### 3. Numerical methods for solution of the coalescence-breakup equation

Eq. (5) with (1), (2), (3) and (4) substituted is integrated numerically, using a procedure originated by Bleck (1970) and modified by Danielsen *et al.* (1972) for improved performance for the pure coalescence problem. The procedure is extended to apply also to the breakup term as defined by Eq. (3).

The mass coordinate is broken up into a set of discrete classes  $m_1, m_2, \dots, m_N$  by choosing  $m_{i+1} = 2^{1/l} m_i$ , where  $l$  is an integer which determines how narrow the classes will be. The extended equation (5) is then averaged over each class interval  $m_i$  to  $m_{i+1}$  using the definition for the averaging process

$$\bar{n}_i(t) = \frac{\int_{m_i}^{m_{i+1}} n(m, t) m dm}{\int_{m_i}^{m_{i+1}} m dm} = \frac{2}{m_{i+1}^2 - m_i^2} \int_{m_i}^{m_{i+1}} n(m, t) m dm. \quad (6)$$

Thus, the continuous drop-size spectrum  $n(m, t)$  is replaced by the discrete values  $\bar{n}_i(t)$  representing mass-weighted average of  $n$  in the interval  $(m_i, m_{i+1})$ . Physical grounds for using the mass-weighted average come from the desire to represent the liquid water content in each interval as closely as possible. The result of this averaging is a set of equations relating the  $\bar{n}_i(t)$  in polynomial fashion:

$$\frac{d\bar{n}_i(t)}{dt} = \frac{2}{m_{i+1}^2 - m_i^2} \left( \sum_{j,k} a_{ijk} \bar{n}_j \bar{n}_k - \bar{n}_i \sum_{k=1}^{N-1} b_{ik} \bar{n}_k \right) + \sum_{j,k=1}^{N-1} p_{ijk} \bar{n}_j \bar{n}_k - \bar{n}_i \sum_{k=1}^{N-1} q_{ik} \bar{n}_k. \quad (7)$$

In these equations, the first two terms govern the change in  $\bar{n}_i(t)$  due to coalescences and are specified in detail in the literature (Bleck, 1970; Danielsen

*et al.*, 1972). The prime denotes summation over a limited range of  $j$  and  $k$ . Each coefficient  $a_{ijk}$  and  $b_{ik}$  is a double integral of the coalescence kernel  $K(\mu, m)$  in a certain region of the  $\mu, m$  plane.

The last two summations in (7) govern the breakup process and represent the extension to Bleck's method presented here. The coefficients are given explicitly by the following triple integrals over volumes in  $(m, \mu, \mu_1)$  space represented by the symbols  $C_{ijk}$  and  $D_{ik}$  defined below:

$$p_{ijk} = \int\int\int_{C_{ijk}} \mu(\mu^{\frac{1}{3}} + \mu_1^{\frac{1}{3}})^2 U(m, \mu, \mu_1) d\mu_1 d\mu dm, \quad (8a)$$

$$q_{ik} = \int\int\int_{D_{ik}} \mu(m^{\frac{1}{3}} + \mu_1^{\frac{1}{3}})^2 U(\mu, m, \mu_1) d\mu_1 d\mu dm, \quad (8b)$$

where

$$U(m, \mu, \mu_1) = (3/4)^{\frac{1}{2}} \pi^{\frac{1}{2}} \rho_w^{-\frac{2}{3}} E_1(\mu, \mu_1) \times [V_T(\mu) - V_T(\mu_1)] P(m; \mu, \mu_1), \quad (8c)$$

$$C_{ijk}: m_i \leq m \leq m_{i+1} \text{ and } m_j \leq \mu \leq m_{j+1} \text{ and } m_k \leq \mu_1 \leq m_{k+1}, \text{ for } k < j, \quad (8d)$$

$$C_{ijj}: m_i \leq m \leq m_{i+1} \text{ and } m_j \leq \mu \leq m_{j+1} \text{ and } m_j \leq \mu_1 \leq \mu, \quad (8e)$$

$$D_{ik}: m_i \leq m \leq m_{i+1} \text{ and } m_1 \leq \mu \leq m_N \text{ and } m_k \leq \mu_1 \leq m_{k+1}, \quad (8f)$$

with  $\rho_w$  the water density. This completes the specification of how the mass coordinate is made discrete in the model. In the calculation of the coefficients  $a_{ijk}$ ,  $b_{ik}$ ,  $p_{ijk}$  and  $q_{ik}$ , from experimental data on collisions, a numerical value is obtained by using Simpson's rule to perform the integrations.

Eq. (7) shows that it would be possible to combine the breakup and coalescence coefficients into a single set ( $a_{ijk}$  with  $p_{ijk}$  and  $b_{ik}$  with  $q_{ik}$ ), thus reducing the number of arithmetic operations required to evaluate  $dn_i/dt$ . This was not done because of the desire to study the effects of coalescence and breakup both separately and combined in order to understand how the two processes interact in shaping the drop-size spectrum.

Integration of the time derivative is done by a simple Eulerian forward-difference scheme

$$\bar{n}_i(t + \Delta t) \approx \bar{n}_i(t) + \frac{d\bar{n}_i}{dt} \Delta t, \quad (9)$$

or substituting from (7) and with the time explicitly

shown

$$\begin{aligned} \bar{n}_i(t + \Delta t) \approx \bar{n}_i(t) + \frac{2}{m_{i+1}^2 - m_i^2} & [\sum'_{j,k} a_{ijk} \bar{n}_j(t) \bar{n}_k(t) \\ & - \bar{n}_i(t) \sum_{k=1}^{N-1} b_{ik} \bar{n}_k(t) + \sum_{\substack{j,k=1 \\ k \leq j}}^{N-1} p_{ijk} \bar{n}_j(t) \bar{n}_k(t) \\ & - \bar{n}_i(t) \sum_{k=1}^{N-1} q_{ik} \bar{n}_k(t)] \Delta t. \quad (10) \end{aligned}$$

The initial condition used to start the numerical scheme (9) is simply the average  $\bar{n}_i$  ( $t=0$ ) calculated from the continuous initial condition

$$\bar{n}_i(t=0) = \frac{2}{m_{i+1}^2 - m_i^2} \int_{m_i}^{m_{i+1}} n_0(m) m dm. \quad (11)$$

Usually the Marshall-Palmer (1948) spectrum  $N_0 e^{-\Lambda D}$  is employed. The boundary conditions on the mass coordinate prevent the loss of water to drop categories smaller than  $m_1$  or larger than  $m_N$ . Thus the mass coordinate conserves liquid water (as does the original continuous form of the equation). Straightforward integration of (7) in this form is equivalent to periodic boundary conditions in the space coordinates, so that any drops falling out of the volume of interest are reinjected through its top boundary. This is a procedure which conserves the liquid water content; to model the situation in a rain shaft, however, one has to conserve the rainfall rate. Keeping the liquid water content constant provides insight into how coalescence and breakup influence the drop sizes independent of complicating effects such as sedimentation and sorting of different drop sizes by wind shear. In this way the effects of the microphysical process of collision are isolated from those of the larger scale dynamics.

#### 4. Experimental data required for the model

The principal input to the model is represented by the fragment probability  $P(m; \mu, \mu_1)$ , the coalescence efficiency  $E_2(m, \mu)$ , and the collision efficiency  $E_1(m, \mu)$ . Finally, a function for the terminal speed difference  $V_T(m) - V_T(\mu)$  is needed.

The data obtained by McTaggart-Cowan and List (1975) were used to determine  $P(m; \mu, \mu_1)$ . The basic information consists of high-speed photographic records of several hundred collisions of pairs of drops falling through air in a roughly vertical direction at their correct terminal speeds. Five different pairs of sizes were used, the small drops diameter being 1.0 or 1.8 mm, the large 3.0, 3.6 or 4.6 mm. Collision/breakups were classified into three types and the fragment distributions for each type determined by counting the "outgoing" drops in various size ranges. Coalescences were not observed for any pairs, except

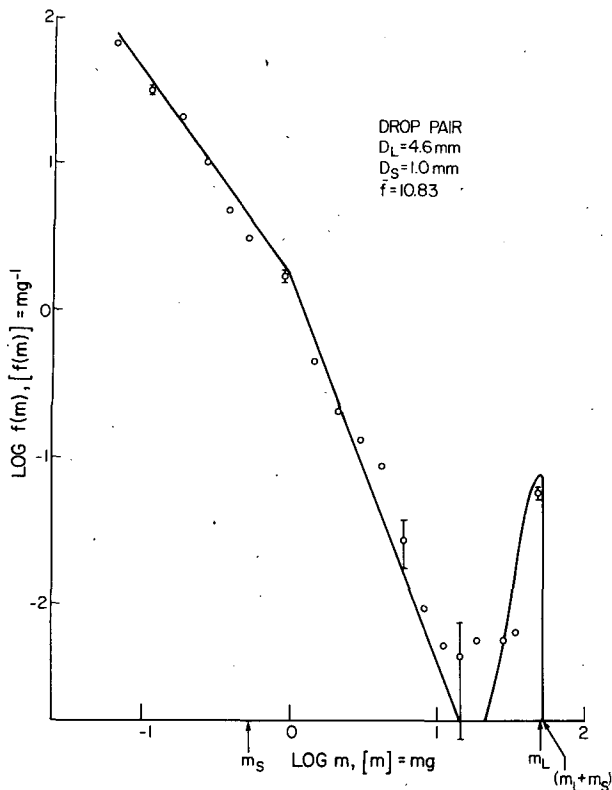


FIG. 1. Observed fragment-size distribution and best-fit curve for modeling. The quantity  $f(m)dm$  is the number of fragments in the mass range  $m$  to  $m+dm$  resulting from a collision between drops of diameters 4.6 mm and 1.0 mm. Circles denote the values observed by McTaggart-Cowan and List (1975). The vertical bars indicate the estimated errors. The solid line shows the values of the interpolating function for the specified diameters of participating drops. The probability function  $P(m; \mu, \mu_1)$  used in the model takes the values of  $f(m)$  when  $\mu$  equals the mass of a 4.6 mm drop and  $\mu_1$  that of a 1.0 mm drop.  $\bar{f}$  is the average fragment number.

1.0 and 3.0 mm, and were quite rare even for those (<5%). The smallest fragments which could be observed had diameters of 0.5 mm.

A typical overall fragment distribution in mass coordinates for collisions of drops with diameters of 4.6 and 1.0 mm, respectively, has a large peak toward the small-fragment end and a smaller peak at the mass of the larger of the participating drops (Fig. 1). For the peak at small  $m$ , a power-law relationship of the form  $P_S(m) = Am^k$  was used as the best choice (compared to  $e^{-m}$  or  $e^{-D}$ ). The parameters to be fitted were the peak value  $n_p$  (at  $m=m_0$ , the lowest mass) and  $\bar{f}$  the total number of small fragments. These are in turn determined from the diameters of the colliding large and small drops  $D_L$  and  $D_S$ , respectively. The observed values are fairly well reproduced and have reasonable behavior in the limits of  $D_S \rightarrow 0$  and  $D_L \rightarrow 0$  with the following description:

$$\bar{f} = 3.6(D_L^3 D_S)^{1/2} (0.41 - 0.30 D_S/D_L), \quad (12)$$

$$n_p = 6.0 \bar{f}/D_S \text{ [equals } n(m=m_0)\text{]}, \quad (13)$$

and the constants of the power law

$$k = -1.0 - 0.392/D_S, \quad A = n_p/0.0654^k, \quad (14)$$

with

$$P_S(m) = (6.0 \bar{f}/D_S)(m/0.0654)^k, \quad \text{if } m \leq 1 \text{ mg} \quad (15)$$

or

$$P_S(m) = (6.0 \bar{f}/D_S)m^{-2.6}/0.0654^k, \quad \text{if } m > 1 \text{ mg}. \quad (16)$$

Diameters are in millimeters, masses in milligrams.

This relationship fits the peak value for each of the five drop pairs observed in M-L within 25% and reproduces the shape of the distributions in general. In almost all cases, the observed points are within a factor of 2 of the calculated values. Because of the property that probability density functions must integrate to unity, errors will tend to compensate.

A similar approach was applied to the large-drop peak. The area under the peak in the observed data was found to be unity. This means that in most collisions a large fragment was formed that was recognizable as the remnant of the participating large drop. In consequence the height and width of the peak at the large-drop mass must be inversely proportional. Using a Gaussian distribution to fit the observed points, the following representation was found for the large fragments with the peak at  $m = m_L$ :

$$P_L(m) = \begin{cases} H \exp[(m - m_L)^2 H^2/2], & \text{if } m \leq m_L + m_S \\ 0, & \text{if } m > m_L + m_S \end{cases} \quad (17)$$

with

$$H = 11.84/[D_L^4 D_S (0.41 - 0.30 D_S/D_L)], \quad (18)$$

and the standard deviation

$$\sigma = H^{-1}. \quad (19)$$

The distribution is cut off for  $m > m_L + m_S$  because no fragment larger than the sum of the incoming masses can be produced.

The overall fragment distribution is then

$$P(m) = P_L(m) + P_S(m). \quad (20)$$

These empirical equations [(12)–(20)] represent the measurements in a continuous fashion and interpolate where no observations are available at this time. The limiting behavior as  $D_S$  and  $D_L$  become small is reasonable for the range of drop diameters considered. The distribution in (20) provides a fragment probability function which can be numerically integrated to give the coefficients in (8).

To obtain the coalescence efficiency, the form proposed by Whelpdale and List (1971) was used, modified to agree with the observed absence of coalescence once the small drop exceeds 1 mm in diameter:

$$E_2(D_L, D_S) = \begin{cases} (1 + D_S/D_L)^{-2}, & D_S \leq 1 \text{ mm} \\ 0, & D_S > 1 \text{ mm} \end{cases} \quad (21)$$

Experiments by M-L led to the conclusion that, for raindrops at least, inertial effects are large enough to prevent the incoming small drop from being deflected noticeably by the flow around the larger one. The drop trajectories are essentially straight lines for these raindrops. Thus the geometrical value  $E_1(D_L, D_S) = 1$  is appropriate. The formula of Best (1950) for the terminal speed for the ICAN standard atmosphere and drop diameters between 0.3 and 6.0 mm is

$$V_T(m) = A \exp(bz) \{1 - \exp[-(m/a_1)^{n_1}]\}, \quad (22)$$

where  $m$  is drop mass (mg),  $A = 9.32 \text{ m s}^{-1}$ ,  $b = 0.0405 \text{ km}^{-1}$ ,  $z = h \text{ [km]}$ ,  $a_1 = 2.90 \text{ mg}$ , and  $n_1 = 0.382$ . This equation is valid for drop masses in the range 0.014–113 mg and agrees with the measurements of Gunn and Kinzer (1949) over that range. Then the difference in terminal speeds becomes

$$\Delta V_T(m_1, m_2) = A \exp(bz) \times \{\exp[-(m_2/a_1)^{n_1}] - \exp[-(m_1/a_1)^{n_1}]\}. \quad (23)$$

**5. Results of the model**

The evolution of a drop-size spectrum, starting with the Marshall-Palmer distribution at a rainfall rate of  $100 \text{ mm h}^{-1}$ , is shown in Fig. 2. Both breaking and coalescence mechanisms are operating, and as is readily apparent the large drops are disappearing very rapidly. The liquid water is redistributed among drops  $< 1.5 \text{ mm}$  diameter. As the integration proceeds to 5 min, the spectrum approaches a limiting slope with the large drops severely depleted and a slope considerably steeper than originally. An idea of the rapidity of this process can be gained if one notes that in 1 min, a drop with diameter 3 mm will fall only 800 m relative to the surrounding air, which is generally small as compared to the raindrop path. Thus drops larger than this will almost certainly not survive a typical fall if smaller drops are present to collide with them.

The initial Marshall-Palmer distribution has approximately 3% of its mass to the left of the cutoff that develops during its evolution. Most of this is captured by larger drops (up to 1.5 mm) in the first 1.5 min. The presence of the cutoff is attributed to the fact that no fragments  $< 0.5 \text{ mm}$  could be observed in the experimental study. Note that the distributions essentially keep their straight line character on a log-linear plot. This means that they all are of the Marshall-Palmer type.

If the straight line portion with negative slope is extrapolated leftward to the  $D=0$  ordinate, then the intercept  $N_0$  may be determined.  $N_0$  increases rapidly with time to a limiting value, reflecting the corresponding decrease in the number of larger drops due to the breakup process. At the same time, the rainfall rate  $R$  decreases (particularly if it was large to begin with)

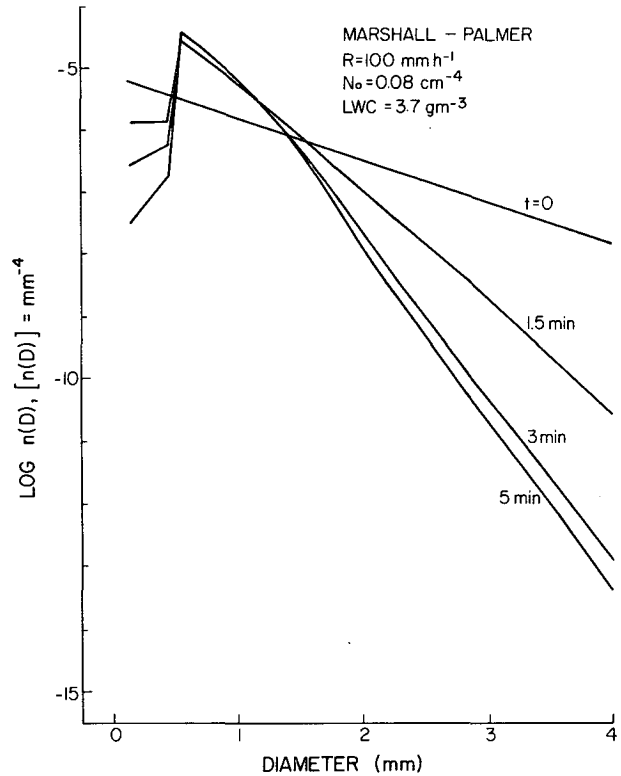


FIG. 2. Time evolution through coalescence and breakup of a raindrop spectrum initially described by a Marshall-Palmer distribution  $n(D) = N_0 \exp(-\Lambda D)$ ,  $\Lambda = 4.1 R^{-0.21}$ , initial  $N_0 = 8 \times 10^{-6} \text{ mm}^{-4}$  and rainfall rate  $R = 100 \text{ mm h}^{-1}$ . Note that the main portion of the spectrum remains approximately linear (Marshall-Palmer) in form while the large drops vanish very quickly through breakup. Small drops are depleted by coalescence. If the straight-line main portion of the spectrum is extrapolated to  $D=0$ , then the intercept  $N_0(t)$  is obtained. The cutoff at  $D=0.5 \text{ mm}$  is due to the limited resolution of the experiment; no particles  $< 0.5 \text{ mm}$  were observed. Only 3% of the drop mass is to the left of the cutoff at  $t=0$ .

because the mean terminal speed of the ensemble of drops is reduced by the loss of the large, fast-falling ones. The two effects are shown in Fig. 3, which illustrates the variation in  $N_0$  and  $R$  for a family of drop spectra. Initially, the spectra all have  $N_0 = 8 \times 10^{-6} \text{ mm}^{-4}$  and varying  $R$  up to approximately  $150 \text{ mm h}^{-1}$ . Solid lines show the  $t=0, 90$  and  $180 \text{ s}$  isochrones and the limiting values as  $t \rightarrow \infty$ . Dashed lines indicate the trajectories of individual spectra. Note the large increase in  $N_0$  for spectra that initially have high rainfall rates. In addition, the rainfall rates decline to limiting values quite rapidly for all members of the family. Both effects reflect the loss of large drops from the spectra with consequent narrowing of the populated size ranges. This narrowing of the spectra occurs without the production of a second peak in the drop-size distribution. Thus the spectra are at all times unimodal [in contrast to the results of Brazier-Smith *et al.* (1973), which tended to be bimodal but did not simulate atmospheric conditions].

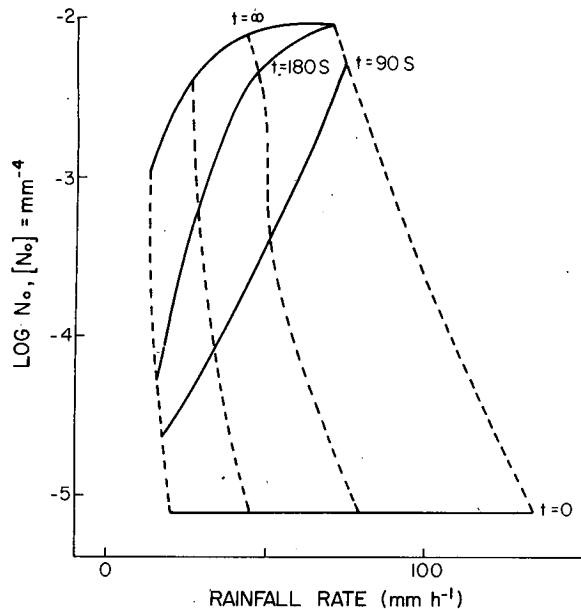


FIG. 3. Evolution of  $N_0$  and rainfall rate  $R$  for a family of Marshall-Palmer distributions. Initially  $N_0$  has the classical value of  $8 \times 10^{-6} \text{ mm}^{-4}$ . Solid curves show values of  $N_0$  and rainfall rate for the family at given times after initiation. Dashed curves give the trajectories of selected members of the family. The very rapid increase in  $N_0$ , especially for distributions with high initial rainfall rate, and the decrease in  $R$  are evident. This reflects the rapid breakup of large raindrops.

## 6. Interpretation of the results

It is perhaps surprising that the majority of large ( $D \geq 3 \text{ mm}$ ) raindrops in the model does not survive for times long enough to fall from a cloud to the ground. However, large raindrops with diameters of 5–6 mm and more are observed in nature. How is this apparent discrepancy explained?

The solution of the dilemma is in the difference between warm and cold rain. Cold rain is formed (by definition according to Wegener-Bergeron-Findeisen) from melting ice particles. These ice particles can grow up to hailstone size by accretion without experiencing breakup in collisions. Hence in their fall to the ground and after passing through the  $0^\circ\text{C}$  level they will start to melt and form large drops. The breakup process will then start from this initial drop-size distribution, and the drops will experience breakup during the fall to the ground. The time of fall may not be sufficient enough to reach an equilibrium drop-size distribution as indicated by Fig. 2.

In contrast to cold rain, there is no source of large drops in warm rain. The ice phase is not present and the breakup process starts to act while the growing drops reach 1–2 mm in diameter. The numerical experiments suggest that it is nearly impossible in warm rain for drops to grow to large sizes ( $D \geq 3 \text{ mm}$ ). If such drops come into existence, they will break up very quickly. This was also proven numerically;

a steady-state distribution was reached through growth by coalescence, slowed down by breakup (an overshooting was observed but cannot be explained satisfactorily at present). Therefore, the hypothesis is that the raindrop sizes in widespread, steady-state tropical rain are considerably smaller than raindrops from showers in middle latitudes. This seems to be commonly observed but records in the scientific literature about warm rain spectra are virtually nonexistent. By inference one can assume that Woodcock and Blanchard (1955) and Blanchard and Spencer (1957) observed warm rain in Hawaii; in a large fraction of the records the largest drops observed for rainfall intensities up to  $33.9 \text{ mm h}^{-1}$  were 2.2 mm. One group of data showed 3.4, 3.8 and 3.2 mm drops at respective rainfall rates of 16.5, 78.0 and  $29.0 \text{ mm h}^{-1}$ . On the other hand, the existence of large drops in cold rain is well established in the literature.

## 7. Limitations of the model and possible refinements

Since the formulation of a physical theory of the breakup probability  $P(m; \mu, \mu_1)$  is far too difficult, it will be necessary to expand the experimental data base. This is especially important for drop sizes smaller than those examined so far. The present experimental data are adequate to model the decay of large drops as in rain formed by the Wegener-Bergeron-Findeisen process. However, the smaller pairs are required to demonstrate more accurately that in the all-water process the growth of large drops to “critical size” does not occur at all.

The model is based on periodic boundary conditions in space. This prevents the escape of large particles from the population by sedimentation, wind shear or other sorting mechanisms, which may lead to the survival of large raindrops. It is obvious that a full-fledged cloud model is required to simulate raindrop growth starting from the formation of a cloud, with a Lagrangian treatment of the drop movement and growth as used by List and Clark (1973).

## 8. Conclusions

The major conclusions for steady-state, wide-range rain are as follows:

1) Drops larger than 2–3 mm, falling in a population of smaller drops typical of natural rain, break up very quickly (within a few minutes). As a result they will vanish from the population in a relatively short distance of fall (e.g.,  $\sim 2 \text{ km}$  for rainfall rates of  $100 \text{ mm h}^{-1}$ ).

2) If the initial drop-size distribution is of the Marshall-Palmer type, the spectrum conserves the Marshall-Palmer linearity.

3) The relative absence of large drops ( $> 2 \text{ mm}$ ) in tropical rain implies that they never grow in the first

place and that the breakup process starts to reduce the growth rate of larger drops as soon as they reach sizes of 1–2 mm.

4) Large drops observed in cold rain produced by the Wegener-Bergeron-Findeisen process are formed from melting ice particles. Breakup is only possible after melting below the 0°C level, where it reduces the number of large drops gradually on their fall to the ground. The original drop distribution may not change much if the time of drop fall does not allow the evolution of the drop spectrum to reach its asymptotic value. There is no shift to larger drop sizes during the fall if the original large drops are > 2–3 mm.

5) The fact that the number of large drops (5–6 mm) diminishes during the fall from a cloud implies that such drops can only be originating from ice particles with diameters > 5 mm, i.e., hailstones, or from large snow flakes which are rather unlikely to occur in showers.

The experiments by McTaggart-Cowan and List (1975) and the modeling reported in this paper make it clear that the usual textbook statements of “critical sizes” of raindrops where breakup occurs (diameter > 5–6 mm) are inadequate. There is *no* critical size in nature, and breakup starts to occur with drops < 2 mm.

Gillespie and List (1976) present a different model of a steady-state vertical rainshaft with sedimentation and a constant flux of rainwater at different altitudes. The results of that model are qualitatively similar to those given here.

While the sophistication of the modeling is far from satisfactory it has nevertheless been possible to produce and underpin new ideas about how raindrop-size spectra may evolve and how breakup can prevent the growth of substantial numbers of large drops. The collision-coalescence mechanism is important for the transformation of cloud droplets into precipitation particles; breakup keeps the resulting raindrops smaller than expected. To what degree the cloud-water-to-rain conversion is affected by the breakup process can only be answered by sophisticated models. First-order estimates do not indicate great changes in the sweep-out of the liquid water by many small drops as compared to fewer large drops. In summary, the “Langmuir chain process” as outlined in the Introduction, is dead.

*Acknowledgments.* The authors are very grateful for the personal communications they received from Drs. A. Waldvogel, P. M. Austin, R. R. Braham and P. Squires about drop-size distributions in warm rain which are in general agreement with the thrust of this paper. The authors also wish to thank the reviewers for their helpful comments.

One of the authors (J. R. G.) is indebted to the Atmospheric Environment Service and the National Research Council of Canada for financial support. These two organizations sponsored these investigations together with the National Severe Storms Laboratory, NOAA, Norman, Okla.

#### REFERENCES

- Berry, E. X., 1967: Cloud droplet growth by collection. *J. Atmos. Sci.*, **24**, 688–701.
- Best, A. C., 1950: Empirical formulae for the terminal velocity of water drops falling through the atmosphere. *Quart. J. Roy Meteor. Soc.*, **76**, 302–311.
- Blanchard, D. C., and A. T. Spencer, 1957: Raindrop measurements during Project Shower. *Tellus*, **9**, 541–552.
- Bleck, Rainer, 1970: A fast, approximative method for integrating the stochastic coalescence equation. *J. Geophys. Res.*, **75**, 5165–5171.
- Brazier-Smith, P. R., S. G. Jennings and J. Latham, 1973: Raindrop interactions and rainfall rates within clouds. *Quart. J. Roy. Meteor. Soc.*, **99**, 260–272.
- Danielsen, E. F., R. Bleck and D. A. Morris, 1972: Hail growth by stochastic collection in a cumulus model. *J. Atmos. Sci.*, **29**, 135–155.
- Gillespie, J. R., and R. List, 1976: Evolution of raindrop size distributions in steady-state rainshafts. *Preprints Intern. Cloud Physics Conf.*, Boulder, Amer. Meteor. Soc., 472–477.
- Gunn, R., and G. D. Kinzer, 1949: Terminal velocity of fall for water droplets in stagnant air. *J. Meteor.*, **6**, 243–248.
- Klett, J. D., 1971: On the breakup of water drops in air. *J. Atmos. Sci.*, **28**, 646–647.
- Komabayasi, M., T. Gonda and K. Isono, 1964: Lifetime of water drops before breaking and size distribution of fragment droplets. *J. Meteor. Soc. Japan*, **42**, 330–340.
- Langmuir, Irving, 1948: The production of rain by a chain reaction in cumulus clouds at temperatures above freezing. *J. Meteor.*, **5**, 175–192.
- List, R., and T. L. Clark, 1973: The effect of particle size distributions on the dynamics of falling precipitation zones. *Atmosphere*, **11**, 179–188.
- , C. F. MacNeil and J. D. McTaggart-Cowan, 1970: Laboratory investigations of temporary collisions of raindrops. *J. Geophys. Res.*, **75**, 7573–7580.
- Magarvey, R. H., and B. W. Taylor, 1956: Free fall breakup of large drops. *J. Appl. Phys.*, **29**, 1129–1135.
- Marshall, J. S., and W. McK. Palmer, 1948: Relation of raindrop size to intensity. *J. Meteor.*, **5**, 165–166.
- McTaggart-Cowan, J. D., and R. List, 1975: Collision and breakup of water drops at terminal velocity. *J. Atmos. Sci.*, **32**, 1401–1411.
- Melzak, Z. A., 1957: A scalar transport equation. *Trans. Amer. Math. Soc.*, **85**, 547–560.
- Mordy, W. A., and E. X. Berry, 1965: Particle growth by coalescence. *J. Atmos. Sci.*, **22**, 340.
- Pruppacher, H. R., and R. Pitter, 1971: A semi-empirical determination of the shape of cloud and rain drops. *J. Atmos. Sci.*, **28**, 86–94.
- Srivastava, R. C., 1971: Size distributions of raindrops generated by their breakup and coalescence. *J. Atmos. Sci.*, **28**, 410–415.
- Twomey, S., 1964: Statistical effects in the evolution of a distribution of cloud droplets by coalescence. *J. Atmos. Sci.*, **21**, 553–557.
- Whelpdale, D. M., and R. List, 1971: The coalescence process in raindrop growth. *J. Geophys. Res.*, **76**, 2836–2856.
- Woodcock, A. H., and D. C. Blanchard, 1955: Tests of the salt-nuclei hypothesis of rain formation. *Tellus*, **7**, 437–448.